Published in final edited form as:
Am J Physiol Cell Physiol. 2007 September ; 293(3): C1003–C1009.

Force suppression and the crossbridge cycle in swine carotid artery

Christopher M. Rembold
Cardiovascular Division, Department of Internal Medicine, University of Virginia Health System, Charlottesville, Virginia

Abstract

Cyclic nucleotides can relax arterial smooth muscle without reductions in crossbridge phosphorylation, a process termed force suppression. There are two potential mechanisms for force suppression: *1*) phosphorylated crossbridges binding to thin filaments could be inhibited or *2*) the attachment of thin filaments to anchoring structures could be disrupted. These mechanisms were evaluated by comparing histamine-stimulated swine arterial smooth muscle with and without forskolin-induced force suppression and with and without latrunculin-A-induced actin filament disruption. At matched force, force suppression was associated with higher crossbridge phosphorylation and shortening velocity at low loads when compared with tissues without force suppression. Shortening velocity at high loads, noise temperature, hysteresivity, and stiffness did not differ with and without force suppression. These data suggest that crossbridge phosphorylation regulates the crossbridge cycle during force suppression. Actin disruption with latrunculin-A was associated with higher crossbridge phosphorylation when compared with tissues without actin disruption. Shortening velocity, noise temperature, hysteresivity, and stiffness did not differ with and without actin disruption. These data suggest that actin disruption interferes with regulation of crossbridge cycling by crossbridge phosphorylation. Stiffness was linearly dependent on stress, suggesting that the force per attached crossbridge was not altered with force suppression or actin disruption. These data suggest a difference in the mechanical characteristics observed during force suppression and actin disruption, implying that force suppression does not mechanistically involve actin disruption. These data are most consistent with a model where force suppression involves the inhibition of phosphorylated crossbridge binding to thin filaments.

Keywords

force suppression; heat shock protein 20; vascular smooth muscle

ARTERIAL SMOOTH MUSCLE CONTRACTION primarily involves stimulus-induced increases in myoplasmic calcium ($[Ca^{2+}]_i$) which induces crossbridge phosphorylation on Ser^{19} of the myosin regulatory light chain (MRLC) via MRLC kinase (reviewed in Ref. 16). Crossbridge phosphorylation can also be increased by stimulus-induced inhibition of MRLC phosphatase (5,25). Increases in crossbridge phosphorylation are felt to be the primary regulator of contraction (17). These processes are termed “activation.”

Relaxation can occur by the following two general mechanisms: *1*) “deactivation” is the reversal of activation involving crossbridge dephosphorylation by either a reduction in $[Ca^{2+}]_i$ or an increase in MRLC phosphatase activity (5,8,18); *2*) “force suppression” is relaxation that occurs while crossbridge phosphorylation levels remain elevated in the presence

Address for reprint requests and other correspondence: C. M. Rembold, Box 800146, Cardiovascular Division, Univ. of Virginia Health System, Charlottesville, VA 22908−0146 (e-mail: crembold@virginia.edu)..

of excitatory stimuli (1,11,22). Phosphorylation of heat shock protein 20 [HSP20, also known as HspB6 (7)] on Ser^{16} (2,3,10,19,29) has been proposed to be the mediator of force suppression (12,19,22).

The mechanism responsible for force suppression is unknown. One hypothesis is that Ser^{16} phosphorylation of HSP20 prevents phosphorylated crossbridges from binding to the thin filament, a process that would reduce force despite high crossbridge phosphorylation values (12,19). One mechanistic explanation for this first hypothesis is that crossbridge binding could be prevented by HSP20 binding to actin in a manner similar to troponin I [TnI; this is based on a sequence homology between HSP20 and the inhibitory region of TnI (19)]. Specifically, an HSP20 peptide [HSP20-(110−121)] shares five identical amino acid residues with a TnI peptide called the inhibitory peptide [the TnI inhibitory peptide inhibits cardiac contraction as well as native TnI (28)]. HSP20-(110−121) binds to actin/tropomyosin filaments, reduces actin-activated myosin S_1 ATPase activity, and relaxes skinned swine carotid arterial smooth muscle (19). Importantly, this first hypothesis predicts that phosphorylated crossbridges would function normally once bound.

A second hypothesis is that Ser^{16}-HSP20 phosphorylation disrupts the attachment of thin filaments to anchoring structures, a process that would interfere with force transmission along the thin filament rather than altering crossbridge interactions (4,26). This second hypothesis predicts that there would be futile crossbridge cycling occurring when phosphorylated crossbridges bind to detached actin filaments.

In this manuscript, these two hypotheses were tested by comparing the mechanical characteristics of swine arterial smooth muscle with and without forskolin-induced force suppression and with and without latrunculin-A-induced actin filament disruption.

MATERIALS AND METHODS

Tissues

Physiological saline solution (PSS) contained (in mM): 140 NaCl, 4.7 KCl, 2 3-[*N*-morpholino] propane sulfonic acid, 1.2 Na_2HPO_4, 1.6 $CaCl_2$, 1.2 $MgSO_4$, 5.6 D-glucose, and 0.02 EDTA, pH adjusted to 7.4 at 37°C. Swine common carotid arteries were obtained and dissected, the endothelium was removed, and the ends were mounted in aluminum foil clips, bathed in PSS at 37°C, and set at L_o, the optimal length for force development (20). Setting length at L_o involved two contractions with 109 mM extracellular K^+ concentration ($[K^+]_o$) PSS where KCl was substituted stoichiometrically for NaCl. The second high $[K^+]_o$ was used to normalize all succeeding contractions (20).

Velocity measurements

Nineteen tissues from 19 different pigs had velocity measured by mounting one end of the tissue to an adjustable-length stationary rod and the other end to the lever arm of an Aurora Scientific model 310B dual-mode lever operated by Dynamic Muscle Control software (Aurora, Ontario, Canada). All releases were performed after setting tissue length to L_o as described above.

Fourteen tissues were evaluated for force suppression. After the equilibration, each tissue was stimulated with 10 μM histamine for 30 min to determine maximal force, and releases were performed. In the first nine tissues, releases were performed at 10-min intervals to loads of 2, 10, 20, and 40% in a random order (%loads were those entered in the Dynamic Muscle Control software). For the last five tissues, releases were performed alternately at 5-min intervals to loads of 10 and 40% starting before the tissue reached goal force and extending beyond goal force. This alternating protocol ensured that all releases were 5 min after a prior release,

allowing for more accurate force matching (see RESULTS). The tissues, already contracted with 10 μM histamine, were relaxed with forskolin (concentration 0.19 ± 0.03 μM) so that sustained force was ~50% of the force induced by 10 μM histamine alone. This forskolin-induced force was called F_{match}. If force deviated >20% from F_{match}, then forskolin concentration was adjusted to attempt to reach F_{match}. After the releases, the histamine and forskolin were washed out for >30 min, and the tissue was recontracted to the same F_{match} with whatever concentration of histamine was required. Releases were then performed in histamine alone. After treatments, tissue wet weight was measured.

Five tissues were evaluated for the effect of actin depolymerization with the alternating 10 and 40% release protocol. After the equilibration, each tissue was stimulated with 10 μM histamine for 30 min to determine maximal force, and releases were performed. The tissue was then contracted to ~50% of the force induced by 10 μM histamine alone with whatever concentration of histamine was required. This force was termed F_{match}. Releases were then performed. Histamine was washed out, and then the tissue was recontracted with 10 μM histamine and relaxed with 6 μM latrunculin-A to interfere with actin filament polymerization. Releases were then performed as force fell to near F_{match}. Because treatment with latrunculin-A inhibited all further contractions, the latrunculin exposure was always the last treatment.

Stiffness measurements

Stiffness, noise temperature, and hysteresivity were measured in nine tissues from nine different pigs with the same mounting, tissue length setting, and apparatus as the velocity experiment described above. Tissues were oscillated with sinusoidal amplitude length changes (0.5% L_o at 0.3, 1, 3, 10, and 30 Hz) and the resulting change in peak to peak force measured (6,9,22a). Stiffness was calculated as the peak-to-peak change in stress (force normalized to cross-sectional area) observed with 10-Hz oscillations (14,24). Noise temperature was calculated as 1 + the least-squares regression slope of ln stiffness as a function of ln oscillation frequency. Hysteresivity was calculated from plots of the change in stress as a function of change in length during 1-Hz oscillations. The intercept of stress with zero on the length axis was calculated for both the stretch and release phase of the oscillation. Hysteresivity was then calculated as the difference between the stretch and release intercept normalized to mean stress (units are fractional).

Biochemical measurements

Crossbridge (Ser^{19}-MRLC) phosphorylation was determined in swine common carotid artery rings mounted isometrically at 1.0 L_o and then treated to obtain similar forces as observed in the velocity and stiffness experiments described above. For Fig. 2, rings were then either *1*) untreated (control), *2*) activated by adding 10 μM histamine for 30 min, *3*) activated by adding 10 μM histamine for 10 min and then relaxed by addition of 0.1−0.2 μM forskolin so sustained force was ~50% of 10 μM histamine force, or *4*) activated by adding 10 μM histamine in PSS for 10 min, and then the histamine concentration was reduced so sustained force was ~50% of 10 μM histamine force. For Fig. 4, rings were treated similarly with the exception of *treatment 3* in which rings were activated by adding 10 μM histamine for 10 min and then relaxed by addition of 6 μM latrunculin-A and waiting until sustained force was ~50% of 10 μM histamine force. At goal force, rings were then frozen in acetone dry ice and homogenized, and the level of crossbridge (Ser^{19}-MRLC) phosphorylation was determined by isoelectric focusing and immunoblotting as described (22). Three dilutions of homogenates were loaded to ensure that the enhanced chemiluminescence detection system was in the linear range (21). Phosphorylation is reported as moles P_i per mole protein.

RESULTS

Comparison of tissues with and without force suppression

A force lower than that expected for a given level of crossbridge phosphorylation is the definition of force suppression. The first goal of this study was to define whether force suppression was associated with either *1*) high shortening velocity as would be expected by the higher crossbridge phosphorylation or *2*) low shortening velocity as would be expected by the lower force. A high shortening velocity would suggest that crossbridge phosphorylation is still regulating crossbridge cycling and that force suppression does not involve abnormal crossbridge cycling. A lower shortening velocity would suggest that force suppression is altering the regulation of crossbridge cycling by crossbridge phosphorylation.

Fourteen swine carotid artery tissues were contracted twice to ~50% of maximal force with the following two protocols: *1*) histamine alone at varying concentrations, i.e., without force suppression and *2*) 10 μM histamine plus varying concentrations of forskolin, i.e., with force suppression. Tissues were then released to four loads, and the resulting shortening was measured. At matched force levels, the velocity at a lower load (mean 20%) was significantly faster with force suppression (0.00563 ± 0.00049 L_o/s, mean ± 1 SE) when compared to without force suppression (0.00405 ± 0.00036 L_o/s, $P = 0.00015$ by paired *t*-test, velocity 1−2 s after release with exponential curve fitting). The velocity at a higher load (mean 51%) did not significantly differ with force suppression (0.00140 ± 0.00019 L_o/s) when compared to without force suppression (0.00132 ± 0.00010 L_o/s, $P = 0.6$ by paired *t*-test). These data suggest that force suppression was associated with more rapid shortening at lower loads as would be expected from the higher MRLC phosphorylation. Figure 1 shows the raw force velocity plot along with its linearized form of all data. Velocities at lower loads were higher with force suppression (histamine plus forskolin) than without force suppression (histamine at matched force). Velocities at higher loads were similar with and without force suppression.

When unloaded velocity was calculated from the initial nine experiments, the linearized Hill plots of the force suppression data did not fit the data well (Fig. 1, *inset*). The *y*-intercept of the linearized Hill plot produces a reasonable V_o for histamine alone, however, the *y*-intercept of the linearized Hill plot was near zero for force suppression, suggesting an unreasonably high calculated unloaded velocity. Upon further data analysis, there were two issues confounding the data: *1*) the first release differed from subsequent releases and *2*) force matching was less accurate with multiple releases. Because obtaining matched force with or without force suppression required a 60- to 90-min treatment, it was impractical to obtain data only on the first release. Therefore, the protocol was altered for the last five tissues such that a high and a low loaded release were performed alternately at 5-min intervals starting prior to force reaching the force matching value. This protocol permitted more precise force matching near ~50% and also ensured that all releases were performed 5 min after a prior release. Specifically, the variation (SD ÷ mean) of the force before release was 5.1% for the initial nine experiments and 0.49% for the final five experiments with the new protocol.

With this new alternating protocol, velocities were similar to the entire data set: at matched force levels, the velocity at the low load (17 ± 0.07%) was significantly faster with force suppression (0.00548 ± 0.00080 L_o/s, mean ± 1 SE) than that observed without force suppression (0.00399 ± 0.00046 L_o/s, $P = 0.05$ by paired *t*-test). The velocity at the high load (48 ± 2.2%) did not significantly differ with force suppression (0.00143 ± 0.00025 L_o/s) when compared to without force suppression (0.00126 ± 0.00012 L_o/s, $P = 0.5$ by paired *t*-test).

Summary biochemical and mechanical data with and without force suppression are shown in Fig. 2. Resting tissues had low crossbridge phosphorylation (MRLCp), high noise temperature, high hysteresivity, low stiffness, and low stress (Fig. 2). Sustained 10 μM histamine-induced

maximal stimulation was associated with high crossbridge phosphorylation, high velocity, low noise temperature, low hysteresivity, high stiffness, and high stress (Fig. 2). Figure 2 also shows the two force-matched states with and without force suppression. Force suppression (histamine plus forskolin; Fig. 2) was associated with significantly higher crossbridge phosphorylation and shortening velocity at low load when compared to tissues without force suppression (histamine alone, Fig. 2). Shortening velocity at high load, noise temperature, hysteresivity, stiffness, and stress did not differ with and without force suppression.

The dependence of velocity on crossbridge (MRLC) phosphorylation is shown in Fig. 3. Velocity was linearly dependent on crossbridge phosphorylation (Fig. 3, *top*), a result similar to prior studies (15). These data are consistent with the hypothesis that crossbridge phosphorylation regulates crossbridge cycling as measured by shortening velocity.

Comparison of tissues with and without actin disruption

Five swine carotid artery tissues were contracted three times: *1*) with maximal histamine (10 μM), *2*) with histamine alone at varying concentrations to ~50% of 10 μM histamine-induced force, i.e., without actin disruption, and *3*) with 10 μM histamine plus 6 μM latrunculin-A to ~50% of 10 μM histamine-induced force, i.e., with actin disruption. Tissues were then alternately released to low and high loads (similar protocol to the last 5 tissues with force suppression). Summary biochemical and mechanical data with and without actin disruption are shown in Fig. 4. Resting tissues had low crossbridge phosphorylation (MRLCp), high noise temperature, high hysteresivity, low stiffness, and low stress (Fig. 4). Sustained 10 μM histamine stimulation was associated with high crossbridge phosphorylation, high velocity, low noise temperature, low hysteresivity, high stiffness, and high stress (Fig. 4). Figure 4 also shows the two force-matched states with and without actin disruption. Actin disruption (histamine + latrunculin-A) had significantly higher crossbridge phosphorylation when compared to tissues without actin disruption (histamine alone; Fig. 4). Shortening velocity, noise temperature, hysteresivity, and stiffness did not differ with and without actin disruption. These data are consistent with the hypothesis that actin disruption produces actin filaments that do not transfer shortening or force to the ends of the tissue (so that phosphorylated crossbridges binding to these actin filaments are functionally inactive). In essence, this hypothesis states that actin disruption results from futile crossbridge cycling when phosphorylated crossbridges bind to thin filaments that are detached from their anchoring structures. These data also suggest that force suppression and actin disruption differ mechanically.

Stiffness is proposed to be an estimate of the number of attached crossbridges. Figure 5 shows a plot of stiffness as a function of stress in all the tissues studied. There was a significant linear dependence of stiffness on stress in tissues that were unstimulated, stimulated with histamine to various forces, with forskolin-induced force suppression, and with latrunculin-A-induced actin disruption ($r^2 = 0.97$). These data suggest that the amount of force per attached crossbridge was not altered with force suppression or actin disruption.

DISCUSSION

The mechanism responsible for force suppression likely involves inhibition of phosphorylated crossbridge binding to thin filaments

This study evaluated two alternative hypotheses. The first was that force suppression involves inhibition of phosphorylated crossbridge binding to thin filaments, a process that would reduce force despite high crossbridge (MRLC) phosphorylation values. The second hypothesis was that force suppression involves disruption in the attachment of thin filaments to anchoring structures, a process that would interfere with force transmission along the thin filament. Overall, the data support the first hypothesis: *1*) If force suppression involved disruption in the

attachment of thin filaments to anchoring structures, then the mechanical characteristics of force suppression should be similar to the mechanical characteristics observed with actin disruption by an agent such as latrunculin-A. However, shortening velocity at low loads with force suppression remained high (that predicted by high crossbridge phosphorylation; Fig. 2) while shortening velocity with latrunculin-A was low (that predicted by lower stress; Fig. 4). These data suggest that force suppression differs mechanically from latrunculin-A-induced actin disruption, a result supportive of the first hypothesis. *2*) If force suppression prevents binding of phosphorylated crossbridges to the thin filament without altering cytoskeletal structure, then force suppression should not alter the dependence of stiffness on stress, noise temperature, or hysteresivity, precisely the result shown in Fig. 2. *3*) If force suppression involved disruption in the attachment of thin filaments to anchoring structures, then there should be increased futile cycling of those crossbridges that attach to disrupted thin filaments. Such futile crossbridge cycling would increase ATP utilization and therefore increase oxygen consumption beyond that expected by the force level. However, nitroglycerin-induced force suppression in swine carotid artery was associated with low oxygen consumption as expected by the reduced stress (19). This finding of low oxygen consumption during force suppression is consistent with the first hypothesis in which reduced crossbridge attachment would be expected to reduce ATP utilization. *4*) It is known that agonist-induced contraction increased the F-actin content in both trachealis and swine carotid artery (12,13), suggesting that contraction is associated with actin polymerization. If the second hypothesis were true, then force suppression may be associated with actin depolymerization (i.e., a decreased F-actin content). However, in the swine carotid artery, force suppression was not associated with a reduction in F-actin content when compared with histamine stimulation alone (12). This result suggests that actin depolymerization does not occur with force suppression, a result supporting the first hypothesis. The finding that noise temperature and hysteresivity did not differ with and without force suppression also appears to support this hypothesis; however, the lack of an effect of latrunculin-A on noise temperature and hysteresivity suggests that these measures may not be sensitive enough measures at this force level (see below). *5*) Finally, the dependence of relaxation on Ser^{16}-HSP20 phosphorylation is linear with forskolin treatment, a result consistent with HSP20-induced reduction of crossbridge binding rather than disruption of entire thin filaments (12). If force suppression were to disrupt entire thin filaments, a sigmoidal dependence of relaxation on Ser^{16}-HSP20 phosphorylation would be expected. If we assume that HSP20 is the mediator of force suppression, this analysis supports the first hypothesis that force suppression is caused by reduction of crossbridge binding.

Why is shortening velocity at low loads high during force suppression?

With force suppression, low-loaded shortening velocity was higher than that observed with histamine alone, despite similar stress (Figs. 1 and 2). The shortening velocity at low loads was high as expected from the higher crossbridge phosphorylation (Fig. 3). This result suggests that crossbridge cycling at low loads is not altered by force suppression. How then does force suppression reduce force? Evaluation of the entire force-velocity relationship could potentially help to explain this confusing result (Fig. 6). A calculation with only two points is not ideal; however, as noted in the results section, poor force matching with multiple releases appeared to result in unphysiologically high calculated V_o. With better force matching, Fig. 6 shows that the higher V at low loads predicted a higher V_o with force suppression compared to without force suppression.

This result could be fit by a hypothesis in which F_o (isometric force) was reduced during force suppression because there were fewer “active” crossbridge binding sites for phosphorylated crossbridges to bind and produce force and/or shortening at high loads. A reduction in active crossbridge binding sites with force suppression could produce “substrate depletion” for crossbridge binding (here actin is the “substrate” for crossbridges binding). Depletion of active

crossbridge binding sites would be most apparent during the relatively slow shortening present when the load is high, since a large number of bound crossbridges are required to produce force; crossbridges would need to rebind frequently given shortening at high loads. This explains the similar velocity at higher loads despite higher crossbridge phosphorylation during force suppression. Substrate depletion would not alter velocity as much at lower loads, since binding of only a small number of phosphorylated crossbridges is required to produce rapid shortening at lower loads. This allows the higher crossbridge phosphorylation during force suppression to produce high unloaded and low-load velocity (Figs. 1, 2, and 6). This hypothesis is consistent with the hypothesis that Ser^{16} phosphorylated HSP20 binds to and inactivates thin filaments so that some of the phosphorylated crossbridges are unable to attach, a process that would reduce force despite high crossbridge phosphorylation values (12,19).

The mechanism of reduced force with actin disruption

With latrunculin-A-induced actin disruption, shortening velocity and stress were similar to that produced by histamine alone despite higher crossbridge phosphorylation (Fig. 6). This result is explained by a hypothesis in which actin disruption produces some thin filaments that are not attached to anchoring structures so that phosphorylated crossbridges attaching to these detached filaments would not induce shortening, stiffness, or stress.

It should not be assumed that all of the effects of latrunculin-A are caused by a direct effect on crossbridge interactions. Cytochalasin B and D, agents that reduce actin polymerization like latrunculin-A, attenuated carbachol-induced increases in $[Ca^{2+}]_i$, crossbridge phosphorylation, and contraction in bovine trachealis (27), suggesting that actin polymerization may be involved in regulation of Ca^{2+}/crossbridge phosphorylation. Our data did not show a statistically significant decrease in crossbridge phosphorylation when comparing 10 μM histamine alone with 10 μM histamine plus 6 μM latrunculin-A ($P = 0.22$); however, the relation of crossbridge phosphorylation and force is steep (23) so that small decreases in crossbridge phosphorylation will decrease force significantly. It is possible that the lack of a significant decrease in crossbridge phosphorylation is a type 2 error.

Implications of noise temperature and hysteresivity

With both force suppression and latrunculin-A-induced actin disruption, noise temperature and hysteresivity were similar to that produced by histamine alone at the same stress (Figs. 2 and 4). This appears to suggest that that both force suppression and latrunculin-A did not alter cell rheology as measured by noise temperature and hysteresivity. However, preliminary results from our laboratory suggest that most of the change in steady-state noise temperature and hysteresivity occurs when force varies from resting to ~50% of maximal (22a). There was only a small change in noise temperature and hysteresivity when force increases from 50 to 100% of maximal values. These data suggest that noise temperature and hysteresivity may not be sensitive enough measures to detect changes in cell rheology with either force suppression or actin disruption occurring when force is reduced by only 50%. Further study of noise temperature and hysteresivity at lower stress levels with force suppression and actin disruption are the subject of further study.

Force suppression and actin disruption do not alter the mechanics of crossbridges once bound

Stiffness was linearly dependent on stress with all treatment protocols (Fig. 5), suggesting that the force per attached crossbridge was not altered with force suppression or actin disruption.

Conclusion

These data suggest that there is a difference in the mechanical characteristics observed during force suppression and actin disruption. This suggests that force suppression does not mechanistically involve actin disruption. Force suppression appears to involve the inhibition of phosphorylated crossbridge binding to thin filaments.

ACKNOWLEDGMENTS

The technical assistance of Melissa Meeks, Shaojie Han, and Marcia Ripley for biochemical assays is appreciated. Arteries were donated by Smithfield, a division of Gwaltney.

GRANTS

This research was supported by National Heart, Lung, and Blood Institute Grant HL-71191.

REFERENCES

1. Bárány M, Bárány K. Dissociation of relaxation and myosin light chain dephosphorylation in porcine uterine muscle. Arch Biochem Biophys 1993;305:202–204. [PubMed: 8342952]
2. Beall A, Bagwell D, Woodrum D, Stoming TA, Kato K, Suzuki A, Rasmussen H, Brophy CM. The small heat shock-related protein, HSP20, is phosphorylated on serine 16 during cyclic nucleotide-dependent relaxation. J Biol Chem 1999;274:11344–11351. [PubMed: 10196226]
3. Beall AC, Kato K, Goldenring JR, Rasmussen H, Brophy CM. Cyclic nucleotide-dependent vasorelaxation is associated with the phosphorylation of a small heat shock-related protein. J Biol Chem 1997;272:11283–11287. [PubMed: 9111032]
4. Dreiza CM, Brophy CM, Komalavilas P, Furnish EJ, Joshi L, Pallero MA, Murphy-Ullrich JE, von Rechenberg M, Ho YSJ, Richardson B, Xu NF, Zhen YJ, Peltier JM, Panitch A. Transducible heat shock protein 20 (HSP20) phosphopeptide alters cytoskeletal dynamics. FASEB J 18:2004.
5. Etter EF, Eto M, Wardle RL, Brautigan DL, Murphy RA. Activation of myosin light chain phosphatase in intact arterial smooth Muscle during nitric oxide-induced relaxation. J Biol Chem 2001;276:34681–34685. [PubMed: 11461918]
6. Fabry B, Maksym GN, Butler JP, Glogauer M, Navajas D, Fredberg JJ. Scaling the microrheologoy of living cells (Abstract). Phys Rev Lett 2001;87:148102. [PubMed: 11580676]
7. Fan GC, Chu GX, Kranias EG. Hsp20 and its cardioprotection. Trends Cardiovasc Med 2005;15:138–141. [PubMed: 16099377]
8. Gerthoffer WT, Murphy RA. Ca2+, myosin phosphorylation, and relaxation of arterial smooth muscle. Am J Physiol Cell Physiol 1983;245:C271–C277.
9. Gunst SJ, Fredberg JJ. The first three minutes: smooth muscle contraction, cytoskeletal events, and soft glasses. J Appl Physiol 2003;95:413–425. [PubMed: 12794100]
10. Jerius JH, Karolyi DR, Mondy JS, Beall AC, Wootton D, Ku D, Cable S, Brophy CM. Endothelial-dependent vasodilation is associated with increases in the phosphorylation of a small heat shock protein (HSP20). J Vas Surg 1999;29:678–684.
11. McDaniel NL, Chen XL, Singer HA, Murphy RA, Rembold CM. Nitrovasodilators relax arterial smooth muscle by decreasing $[Ca^{2+}]_i$, $[Ca^{2+}]_i$ sensitivity, and uncoupling stress from myosin phosphorylation. Am J Physiol Cell Physiol 1992;263:C461–C467.
12. Meeks M, Ripley ML, Jin Z, Rembold CM. Heat shock protein 20-mediated force suppression in forskolin-relaxed swine carotid artery. Am J Physiol Cell Physiol 2005;288:C633–C639. [PubMed: 15509660]
13. Mehta D, Gunst SJ. Actin polymerization stimulated by contractile activation regulates force development in canine tracheal smooth muscle. J Physiol (Lond) 1999;519:829–840. [PubMed: 10457094]
14. Meiss RA. Influence of intercellular tissue connections on airway muscle mechanics. J Appl Physiol 1999;86:5–15. [PubMed: 9887107]

15. Murphy RA, Aksoy MO, Dillon PF, Gerthoffer WT, Kamm KE. The role of myosin light chain phosphorylation in regulation of the cross-bridge cycle. Fed Proc 1983;42:51–56. [PubMed: 6848378]

16. Murphy RA, Rembold CM. The latch-bridge hypothesis of smooth muscle contraction. Can J Physiol Pharmacol 2005;83:857–864. [PubMed: 16333357]

17. Ratz PH, Hai CM, Murphy RA. Dependence of stress on cross-bridge phosphorylation in vascular smooth muscle. Am J Physiol Cell Physiol 1989;256:C96–C100.

18. Rembold CM. Relaxation, $[Ca^{2+}]_i$, and the latch-bridge hypothesis in swine arterial smooth muscle. Am J Physiol Cell Physiol 1991;261:C41–C50.

19. Rembold CM, Foster B, Strauss JD, Wingard CJ, Van Eyk JE. cGMP mediated phosphorylation of heat shock protein 20 may cause smooth muscle relaxation without myosin light chain dephosphorylation. J Physiol (Lond) 2000;524:865–878. [PubMed: 10790164]

20. Rembold CM, Murphy RA. Myoplasmic $[Ca^{2+}]$ determines myosin phosphorylation in agonist-stimulated swine arterial smooth muscle. Circ Res 1988;63:593–603. [PubMed: 3409490]

21. Rembold CM, O'Connor MJ. Caldesmon and heat shock protein 20 in nitroglycerin- and magnesium induced relaxation of swine carotid artery. Biochim Biophys Acta 2000;1500:257–264. [PubMed: 10699367]

22. Rembold CM, O'Connor MJ, Clarkson M, Wardle RL, Murphy RA. HSP20 phosphorylation in nitroglycerin- and forskolin-induced sustained reductions in swine carotid media tone. J Appl Physiol 2001;91:1460–1466. [PubMed: 11509549]

22a. Rembold, CM.; Tejoni, AD.; Ripley, ML.; Shaojieo, Han. Paxillin phosphorylation, actin polymerization, noise temperature, and the sustained phase of swine carotid artery contraction.. Am J Physiol Cell Physiol. Jun 27. 2007 doi:10.1152/ajpcell. 00090.2007

23. Rembold CM, Wardle RL, Wingard CJ, Batts TW, Etter EF, Murphy RA. Cooperative attachment of cross bridges predicts regulation of smooth muscle force by myosin phosphorylation. Am J Physiol Cell Physiol 2004;287:C594–C602. [PubMed: 15151901]

24. Rhee AY, Brozovich FV. The smooth muscle cross-bridge cycle studied using sinusoidal length perturbations. Biophys J 2000;79:1511–1523. [PubMed: 10969012]

25. Somlyo AP, Somlyo AV. Signal transduction by G-proteins, Rho-kinase and protein phosphatase to smooth muscle and non-muscle myosin II. J Physiol (Lond) 2000;522:177–185. [PubMed: 10639096]

26. Tessier D, Komalavilas P, Panitch A, Joshi D, Brophy CM. The small heat shock protein (HSP) 20 is dynamically associated with the the actin cross-linking protein actinin (Abstract). J Surg Res 2003;111:157.

27. Tseng S, Kim R, Kim T, Morgan KG, Hai CM. F-actin disruption attenuates agonist-induced $[Ca^{2+}]$, myosin phosphorylation, and force in smooth muscle. Am J Physiol Cell Physiol 1997;272:C1960–C1967.

28. Van Eyk JE, Hodges RS. The biologic significance of each amino acid residue of the troponin I inhibitory sequence 104–115 in the interaction with troponin C and tropomyosin-actin. J Biol Chem 1988;263:1726–1732. [PubMed: 3338991]

29. Woodrum DA, Brophy CM, Wingard CJ, Beall A, Rasmussen H. Phosphorylation events associated with cyclic nucleotide-dependent inhibition of smooth muscle contraction. Am J Physiol Heart Circ Physiol 1999;276:H931–H939.

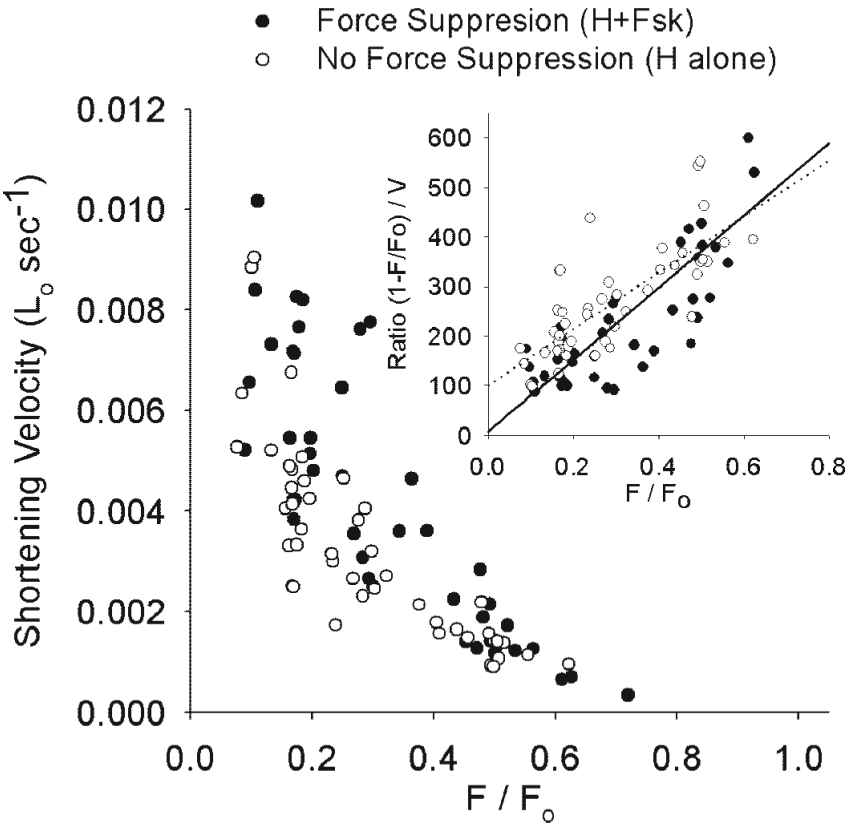

Fig. 1.

Raw data showing higher shortening velocity with force suppression than that observed without force suppression. Swine carotid tissues were either stimulated with 10 μM histamine and relaxed with forskolin to ~50% of maximal force (with force suppression, ●) or stimulated with various concentrations of histamine to the same ~50% of maximal force (without force suppression, ○) and then released to varying afterloads. The *inset* shows the linearized form of the Hill plot (solid line with force suppression and dotted line without force suppression).

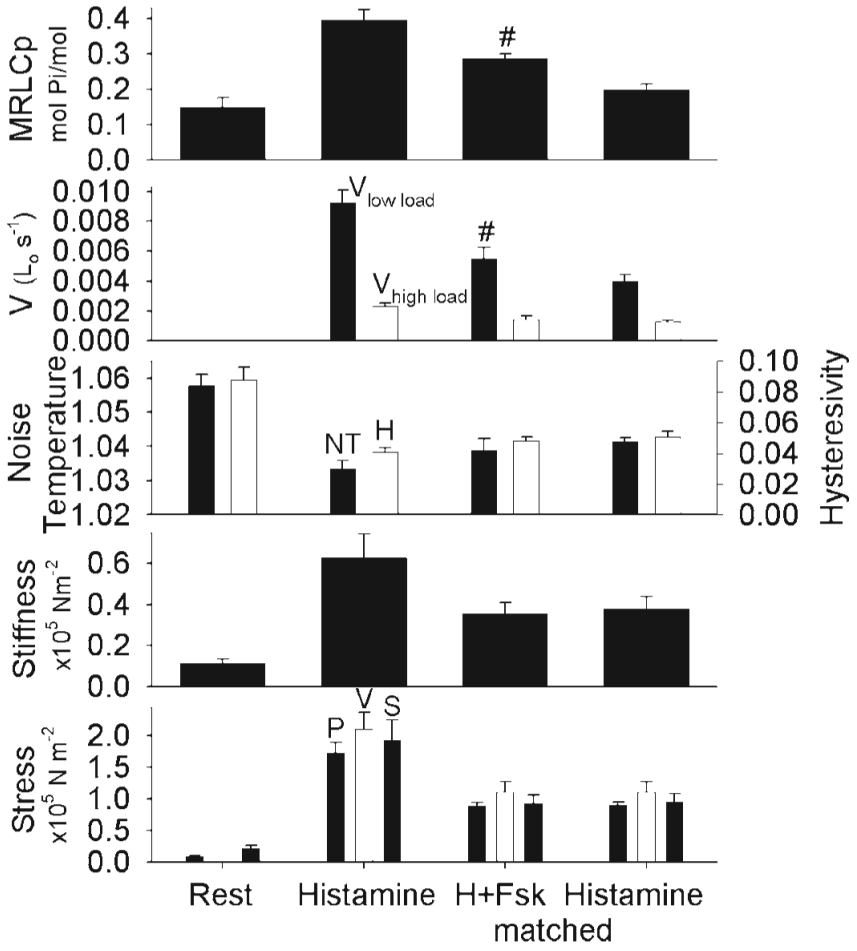

Fig. 2.

Mean biochemical and mechanical characteristics in swine carotid artery tissues with and without force suppression. Tissues were either unstimulated (*column 1*), maximally stimulated with 10 μM histamine for 25− 40 min (*column 2*), stimulated with 10 μM histamine and relaxed with forskolin to ~50% of maximal force (varying times and forskolin concentrations, *column 3*, with force suppression), or stimulated with various concentrations of histamine to the same ~50% of maximal force (*column 4*, without force suppression). The panels shown mean ± 1 SE for crossbridge phosphorylation [phosphorylated myosin regulatory light chain (MRLCp), *panel 1*], shortening velocity at low 17% load (*panel 2*, filled bars labeled "$V_{low\ load}$"), shortening velocity at high 48% load (*panel 2*, open bars labeled "$V_{high\ load}$"), noise temperature (*panel 3*, filled bars), hysteresivity (*panel 3*, open bars), stiffness (*panel 4*), and stress [*panel 5*, the filled bars on *left* (labeled "P") are the stress values from the MRLCp experiments and the open bars (labeled "V") are the stress from the velocity experiments; filled bars on *right* (labeled "S") are from the stiffness experiments]. Data are presented as means ± 1 SE with $n = 5-6$ experiments. #Significant difference when comparing tissues with and without force suppression, i.e., *column 3* vs. *column 4*. Force suppression was associated with significantly higher crossbridge phosphorylation and velocity at low loads when compared to tissues at matched force without force suppression. Velocity at higher load, noise temperature, hysteresivity, and stiffness did not significantly differ with and without force suppression.

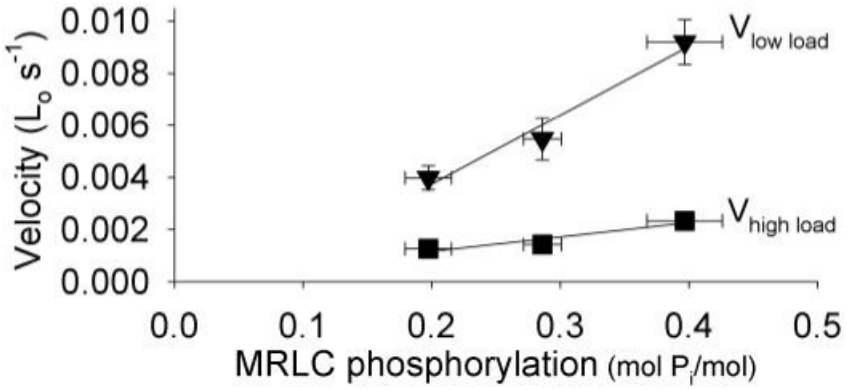

Fig. 3.

Dependence of velocity on crossbridge phosphorylation in swine carotid artery tissues with and without force suppression. Data from Fig. 2 are replotted for comparison. There is a clear dependence of shortening velocity on crossbridge (MRLC) phosphorylation.

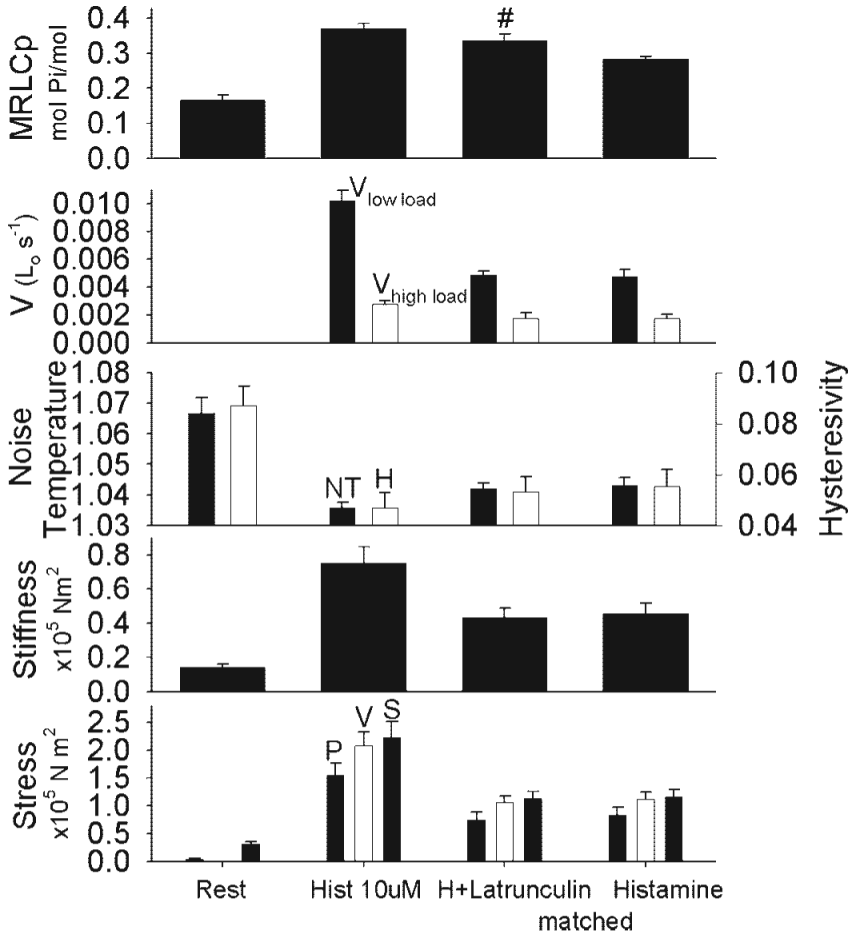

Fig. 4.

Mean biochemical and mechanical characteristics in swine carotid artery tissues with and without latrunculin-A-induced actin disruption. Tissues were either unstimulated (*column 1*), maximally stimulated with 10 μM histamine for 25−40 min (*column 2*), stimulated with 10 μM histamine and relaxed with 6 μM latrunculin-A to ~50% of maximal force (*column 3*), or stimulated with various concentrations of histamine to the same ~50% of maximal force (*column 4*). The panels shown mean ± 1 SE for crossbridge (MRLC) phosphorylation (*panel 1*), shortening velocity at low load (*panel 2*, filled bars labeled $V_{low\ load}$), shortening velocity at high load (*panel 2*, open bars labeled $V_{high\ load}$), noise temperature (*panel 3*, filled bars), hysteresivity (*panel 3*, open bars), stiffness (*panel 4*), and stress (*panel 5*, filled bars on *left* are the stress from the MRLC phosphorylation experiments, the open bars are the stress from the velocity experiments, and the filled bars on *right* are from the stiffness experiments). Data are presented as mean ± 1 SE with $n = 4–6$ experiments. #Significant difference when comparing tissues with and without actin disruption, i.e., *column 3* vs. *column 4*. Latrunculin-A treatment was associated with higher crossbridge phosphorylation when compared to tissues without latrunculin-A treatment at the same force. Velocity, noise temperature, hysteresivity, and stiffness did not significantly differ with and without latrunculin-A treatment.

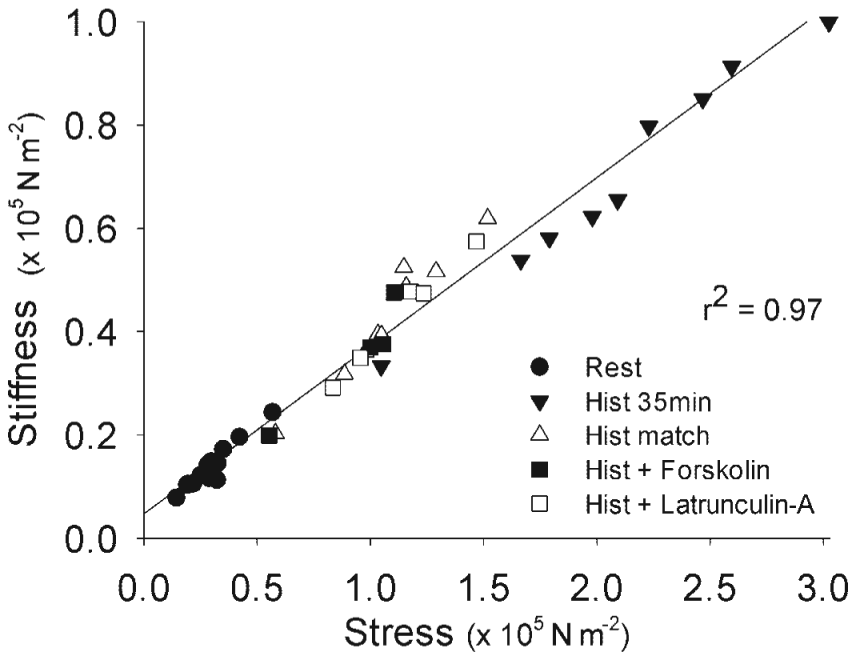

Fig. 5.

Stiffness is linearly dependent on stress regardless of treatment. Raw stiffness and stress data from the above experiments are replotted as noted. Regression was highly significant with $r^2 = 0.97$.

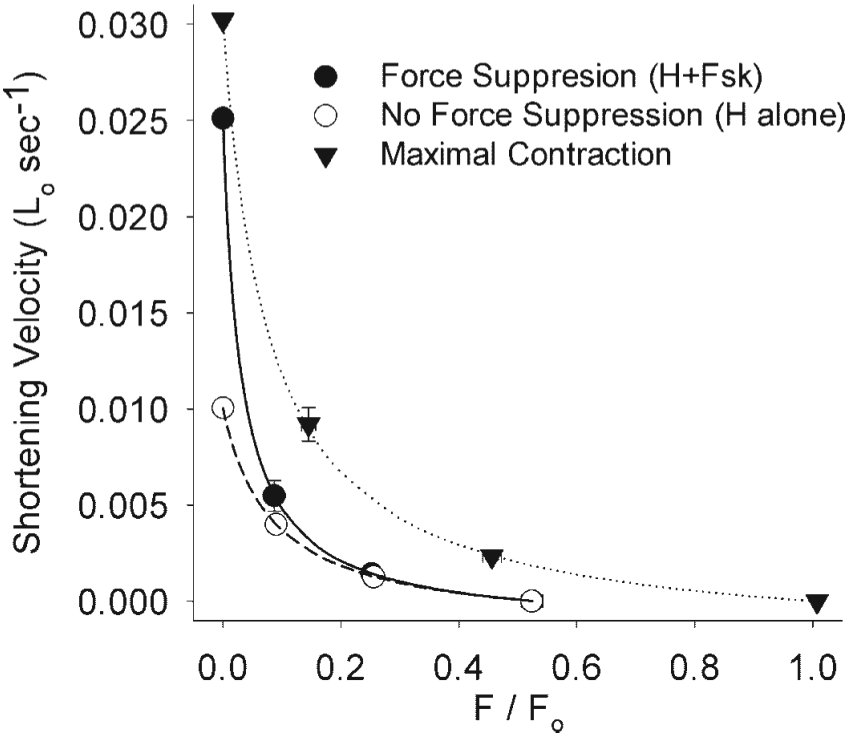

Fig. 6.

Force-velocity relation with (●) and without (○) force suppression. Mean ± 1 SE data from the alternating release protocol (shown in Fig. 2) are replotted along with data from maximal histamine stimulation (▲). The lines result from fitting the raw data to a standard Hill plot. The higher velocity at a low load (F/F_o ~0.08) with force suppression predicts a higher unloaded velocity (V_o at $F/F_o = 0$) despite a similar velocity at higher load (F/F_o ~0.28) and similar isometric force (F/F_o ~0.50 at 0 velocity).